Facile fabrication of 3D graphene hydrogel (rGH) for enhanced removal of heavy metal Cr (VI)

Y. Li[a,b] , X. Y. Zhao[c], X. C. Guo[d] , J. Wang[d] , W. Chen[a,*]
[a]*North China University of Science and Technology, College of Metallurgy and Energy, Hebei Provincial High-Quality Steel Continuous Casting Engineering Technology Research Center, Tangshan Hebei 063210*
[b]*North China University of Science and Technology，Comprehensive test and Analysis Center，Tangshan Hebei 063210*
[c]*Tangshan Open University ,Tangshan Hebei 063210*
[d]*North China University of Science and Technology，Yisheng College，Tangshan Hebei 063210*[1]

The reduced graphene hydrogel (rGH) was prepared by chemical reduction method, and removal performance of heavy metal Cr (VI) in static water was studied. The rGH has a three-dimensional structure and narrow pore size distribution, that the adsorption process of Cr (VI) by rGH is in accordance with Langmuir isotherm model, and the maximum adsorption capacity is 139.6 mg • g^{-1}.The significant adsorption capacity is mainly attributed to the fact that rGH has nano-sheet structure, and maintains the surface adsorption characteristics of graphene with rapid adsorption. The π-π action will reduce the competitive adsorption of water and increase the adsorption capacity.

(Received January 19, 2023; Accepted April 6, 2023)

Keywords: Graphene hydrogel (rGH), Adsorption, Reduction, Cr(VI)

1. Introduction

Chromium (VI) has the characteristics of high toxicity, bioaccumulation, difficult degradation, stable chemical properties and easy to cause biological carcinogenic mutation[1].The pollution of heavy metal ions in water, especially chromium (VI) ions, is becoming more and more serious, which poses a serious threat to human health and ecological security. At present, the main treatment methods of chromium (VI) in wastewater include ion exchange method[2], neutralization precipitation method[3], electrochemical reduction method[4], membrane separation method[5], adsorption method[6], etc.

Graphene is a lamellar carbon material with high specific surface area[7], which has very high adsorption capacity. Graphene has unique characteristics of nonporous surface adsorption and π - π conjugate adsorption[8],compared with porous and interlayer adsorption materials, graphene has the characteristics of fast adsorption and enrichment of heavy metal ions in water and high adsorption strength. In recent years, graphene adsorption for the purification of heavy

* Corresponding author: hblgdxzzb@163.com
https://doi.org/10.15251/DJNB.2023.182.463

metal Cr(VI) has been reported extensively at home and abroad[9,10], which shows the great application potential of graphene in the treatment of heavy metal ions. Therefore, carrying out graphene hydrogel adsorption for the removal of heavy metal ions Cr from water will promote the application of graphene in environmental purification.

In this study, rGH was prepared by chemical reduction, its porous through-net structure and surface adsorption characteristics provide a better movement channel and sites for the adsorption of heavy metal Cr (VI), improve ion diffusion and reduce mass transfer resistance, it will exhibit excellent characteristics such as fast adsorption rate and high adsorption capacity.At the same time, the surface of the adsorption material retains abundant functional groups and has good chemical stability. It was studied the effects of initial concentration, time, temperature, ionic strength and pH of solution on the removal effect of heavy metal Cr (VI) in water, and discussed the adsorption kinetics, thermodynamics and adsorption isotherm of the adsorption process.

2. Experimental

2.1. Preparation of graphene hydrogel (rGH) adsorbent materials

Add 3.0 g of graphite (325 mesh) to 70 ml of concentrated sulfuric acid in an ice bath and stir for 10 minutes, then add 1.5 g of sodium nitrate and 9 g of potassium permanganate (3 times as much as graphite), stir for 2.5 hours and avoid the temperature of the reaction system above 20ºC. Then raise the temperature of the system to 35 ºC for 3.5 hours, then add 150 mL of deionized water and raise the temperature of the system to 95 ºC. Continue stirring for 1.5 hours, then 300 ml of deionized water and 20 ml (30%) of hydrogen peroxide were added successively, and then the reactants were washed with dilute hydrochloric acid, centrifuged and dialyzed to obtain graphene oxide (Go).

Graphene oxide was reduced using a certain amount of ascorbic acid (VC), and graphene hydrogels (rGH) were prepared by chemical reduction in a water bath at 95°C for 60 min.

2.2. Characterization of reduced graphene oxide hydrogel (rGH) adsorbent materials and determination of adsorption

The phase of the sample was analyzed by D / MAX2500pc X-ray diffractometer (XRD) of Japanese science; S-4800 field emission scanning electron microscope (SEM) of Hitachi was used to observe the micro morphology of the adsorption material; Hitachi ht-7700 (Transmission electron microscope TEM) was used to analyze the morphology and size of the samples; The information of atomic structure and electronic properties was measured by DXR laser Raman spectrometer (Raman) of American thermal power company.

2.3. Characterization of adsorption properties of graphene hydrogel (rGH) materials

Static adsorption performance of rGH hydrogels:The objective of this study is to evaluate the adsorption performance of rGH hydrogel. The target pollutant is $K_2Cr_2O_7$ (Cr (VI)), which is dissolved in Wahaha pure water and made into 200 mgL^{-1} stock solution for sealing storage.The adsorption experiments is performed as follows: 100 mg rGH hydrogel is placed in a 250 mL conical flask with a stopper, and a 100 mL concentration of Cr (VI) solution is added. Then the

conical flask is placed into SHZ-88A type reciprocating water bath constant temperature oscillation, the oscillation speed is 200 r·min^{-1}, and the adsorption experiment is carried out at a certain temperature, sampling were taken at regular intervals (3 mL) and filtering with 0.45 μm filter membrane. The concentration of Cr in the solution was determined using an inductively coupled direct reading spectrometer (ICP) type ULTIMA2 from HORIBA Jobin Yvon, France.

2.4. Processing of data from static adsorption experiments

(1)Adsorption kinetics

The adsorption capacity q_t of the adsorbent on the target sorbent is calculated as follows:

$$q_t = \frac{(C_0 - C_t)V}{m} \tag{1}$$

where C_0 and C_t respectively refer to the concentration of adsorbate (mgl^{-1}) in the solution in the initial state and at different time state t, V refers to the volume of the solution (L), and m refers to the amount of adsorbent (g).

The desorption rate η of the sorbent to the target sorbent is calculated as follows:

$$\eta = \frac{C_t V}{q_e m} \times 100\% \tag{2}$$

where C_t refers to the concentration of adsorbate in the solution at different time states t(mgl^{-1}), q_e refers to the adsorption capacity of adsorbent to target adsorbate at equilibrium state (mgg^{-1}), V refers to the volume of solution (L), and m refers to the amount of adsorbent (g).

The study of the effect of time on adsorption performance, the kinetic behaviour of adsorption, enables the rate of adsorption of the adsorbent to be determined and the time required for the completion of the adsorption reaction to be determined, and the kinetic data is usually modelled using two models, the quasi primary kinetic equation and the quasi secondary kinetic equation.

(2)Adsorption isotherm

The effect of target adsorbate concentration on adsorption is usually examined in terms of the adsorption isotherm. The adsorption of adsorbent on target adsorbate follows the mathematical law reflected by the adsorption isotherm equation. Langmuir and Freundlich isotherm models are usually used to describe the relationship between the equilibrium concentration of target adsorbate and the equilibrium adsorption capacity of adsorbent in solution at constant temperature.

(3)Adsorption thermodynamics

Thermodynamic parameters can provide deep-seated information on internal energy changes related to adsorption. The standard Gibbs free energy change (△G°), the standard enthalpy change (△H°) and standard entropy change (△S°) are calculated from the

temperature-dependent adsorption isotherms and reflect the state of the adsorption process. The calculation formula of standard Gibbs free energy variation (△G°) is calculated as follow[11]:

$$\Delta G^{\circ} = -RT \ln K^{\circ} \tag{3}$$

where R refers to the gas constant (8.314 $jmol^{-1}k^{-1}$) and T refers to the thermodynamic temperature (K).

3. Discussion and results

3.1. Characterization of graphene hydrogel (rGH)

In Fig.1 shows the XRD spectra of graphite, graphene oxide (GO) and graphene hydrogel (rGH). Graphite in Figure at 2 θ= 26.4 ° shows a sharp and strong diffraction peak, that is, the diffraction peak of graphite 002 surface, and the corresponding crystal plane spacing is 0.34nm. It can be seen that the spatial arrangement of pure graphite microcrystalline layers is very regular. With the oxidation of graphite, the typical 002 graphite diffraction peak does not appear in GO, but in 2 θ=12.1° , a new 001 diffraction peak appears, the corresponding crystal plane spacing is 0.76 nm, indicating that the O in the strong oxidant is bonded with the C atom in the graphite, and a large number of oxygen-containing groups (such as hydroxyl, carbonyl, epoxy, etc.) are introduced at the upper, lower and edge of the graphite sheet, which significantly increases the layer spacing and turns into a GO sheet. Under the reduction of VC, with the decrease of oxygen-containing groups on the GO surface, the layer spacing will decrease accordingly, which is consistent with the change of XRD of graphene, the 002 diffraction peak shifts left to 2θ =24.5°, the corresponding crystal surface layer spacing is 0.36nm, slightly larger than the layer spacing of graphite, indicating that after chemical reduction of rGH, the oxygen-containing groups on the surface are not completely removed, but still partially remain on the graphite flake layer. The 002 diffraction peak intensity of graphene is weakened and widened, indicating that it has changed from the original larger graphite body shape to the smaller graphene sheet flake.

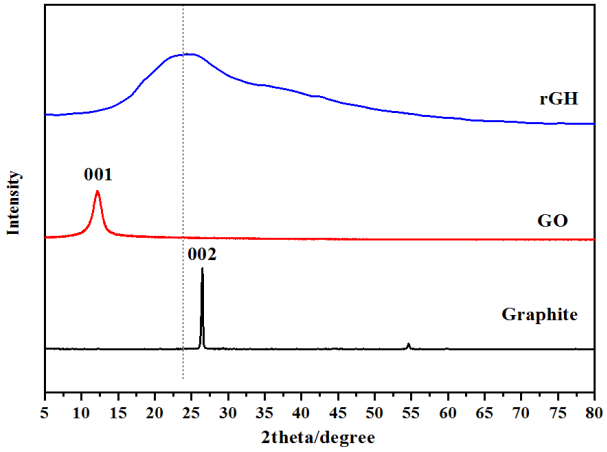

Fig. 1. XRD patterns of Graphite, GO and rGH.

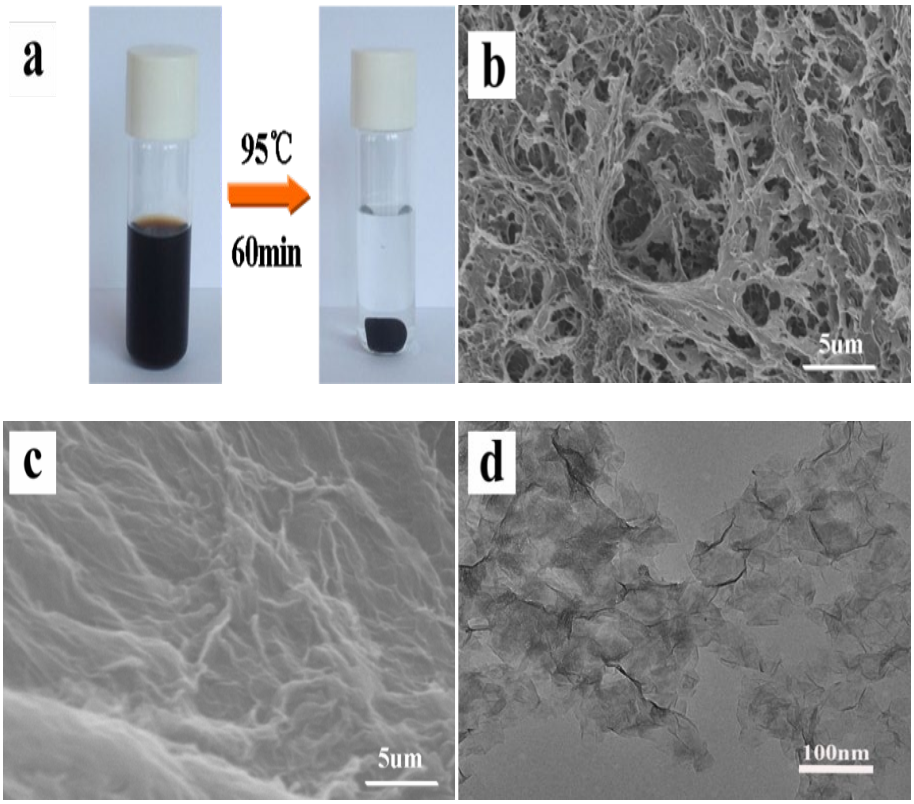

Fig. 2. SEM images for the rGH and Graphene ; TEM images for the rGH.

The structure and morphology of rGH and graphne were analyzed by field emission scanning electron microscope (SEM). Figure a and b show the rGH prepared by chemical reduction method after the reduction of GO with a certain amount of ascorbic acid (VC) and reaction in 95 ℃ water bath for 60 min. From the SEM image, it can be seen that the three-dimensional network microstructure of rGH and the uniform dispersion of several micron sized pores are mainly due to the hydrophobic effect and intermolecular force generated by π-π conjugation between graphene layers. Figure c shows graphene prepared by hydrothermal method, the graphene is edge curled and folded morphology and the graphene flakes appear to re-stack. In comparison, rGH, relying on its porous through network structure and surface adsorption structure, will greatly reduce the mass transfer resistance of ion diffusion in the treatment of heavy metal Cr (VI) in water, provide a better movement channel and place for the adsorption of heavy metal Cr (VI), and show the excellent characteristics of fast adsorption rate and high adsorption capacity. Figure d is the TEM diagram of rGH, which can be seen that rGH shows a gauze-like lamellar structure.

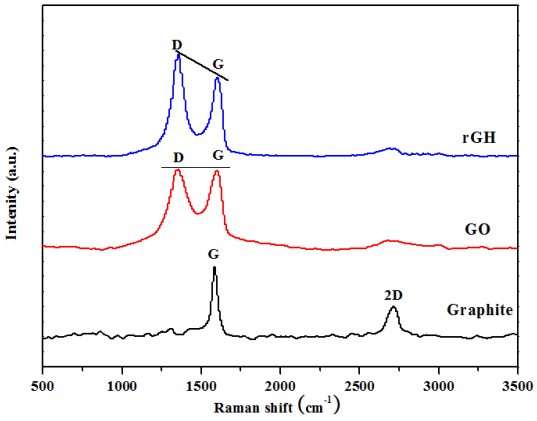

Fig. 3. Raman spectra of the graphite, GO and rGH.

Fig. 3 Raman diagram of graphite, GO and rGH. There is a sharp and strong absorption peak (G peak) in graphite exists at 1584cm^{-1}, which corresponds to the first-order Raman scattering of E2g optical mode, indicating that the structure of graphite is relatively regular. There is a small peak (2D peak) at 2716 cm^{-1}, which is a two phonon resonance Raman peak. After the graphite is oxidized, the G peak of GO has widened and shifted to 1595 cm^{-1}, and a new strong absorption peak (D peak) appears at 1348 cm^{-1}. The corresponding intensities are I_G and I_D respectively, and I_D /I_G is 1.02, indicating that after the graphite is oxidized, part of the SP^2 hybridised carbon atoms in the structure are transformed into SP^3 hybridised structure, the C = C double bond in the graphite layer is destroyed. When GO is reduced, the Raman spectrum of rGH also contains peak positions similar to those of graphene oxide. The intensity ratio of D and G peaks in the Raman spectrogram of rGH is higher than that of graphene oxide, with an I_D/I_G of 1.1, indicating that the number of sp^2 hybridized carbon atoms in rGH is more than that of sp^3 hybridized carbon atoms, the average size of sp^2 hybridized carbon layer plane in rGH is larger than that of GO. After GO is reduced, the structure of rGH is still different from that of graphite.

3.2. Study of Cr(VI) removal by rGH adsorption

Fig. 4 compares the adsorption and purification capacity of rGH and traditional adsorption material activated carbon for Cr (VI) in water. It can be seen that the adsorption process of activated carbon for Cr (VI) is relatively slow, the adsorption takes a long time to reach equilibrium, and it basically reaches equilibrium after 150 min in the equilibrium state, the adsorption capacity of activated carbon is about 25.41mg.g^{-1}. In contrast, within 60 min at the beginning of the reaction, the adsorption capacity of rGH for Cr (VI) increased rapidly, and then reached equilibrium. In the equilibrium state, the adsorption capacity of rGH was about 47.25 mg.g^{-1}.The equilibrium adsorption capacity of rGH is 1.86 times that of activated carbon. At the same time, the experimental data were fitted and analyzed with two models of the pseudo-first-order model simulation and the pseudo-second-order model simulation(Table 1). The theoretical calculated value of adsorption capacity in the fitted equilibrium state was close to the experimental value (q_e). During the adsorption process, the initial adsorption rate h and adsorption rate constant k_2 of rGH were greater than the h and k_2 values for activated carbon.

rGH has nano sheet structure and maintains the surface adsorption characteristics of graphene. Compared with porous and interlayer adsorption materials, rGH avoids the diffusion speed of heavy metal ions in pores and channels during the adsorption process, and has rapid adsorption and enrichment capacity ability. π - π action will reduce the competitive adsorption of water and improve the adsorption capacity.

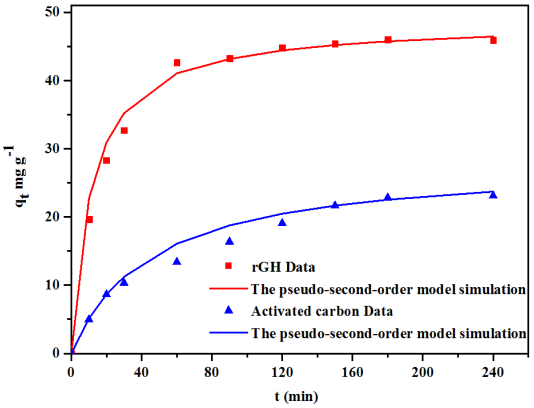

Fig. 4. Effect of contact time on the adsorption of Cr(VI) by graphene and Activated Carbon.

Table 1. Kinetic Parameters for the Adsorption of Cr(VI) by rGH and Activated Carbon.

C_0	$q_{e,cal}$	The pseudo-first-order model simulation			The pseudo-second-order model simulation			
60mg/L	(mg.g^{-1})	k_1	$q_{e,cal}$	R^2	k_2	$q_{e,cal}$	h	R^2
		(h^{-1})	(mg.g^{-1})		(g.mg^{-1}.h^{-1})	(mg.g^{-1})	(mg.g^{-1}h^{-1})	
rGH	47.25	0.020	20.72	0.84	1.8×10^{-3}	48.64	4.25	0.999
Activated carbon	25.40	0.011	15.02	0.82	7.9×10^{-4}	28.18	0.62	0.990

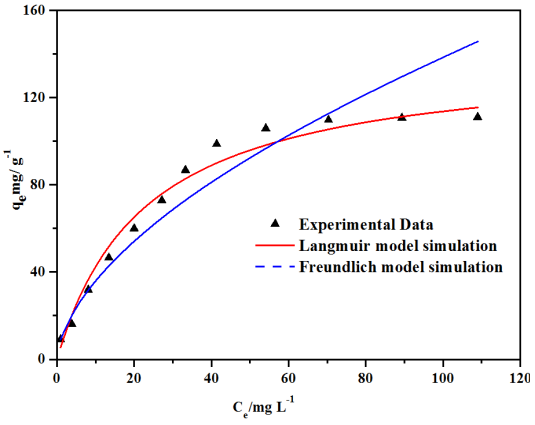

Fig. 5. Adsorption isotherm of the rGH for removal of Cr(VI).

We investigated the adsorption isotherms using heavy metal Cr(VI) solutions with initial concentrations of 10, 20, 40, 60, 80, 100, 120, 140, 160, 180, 200 and 220 mgL^{-1} and water baths set at 10, 30 and 50 °C. After 60 minutes of adsorption reaction, samples were taken to determine the residual concentrations of different Cr (VI) solutions. The obtained experimental data were drawn into the adsorption isotherm curve of rGH equilibrium adsorption capacity q_e and Cr (VI) solution equilibrium concentration Ce, and the experimental data were fitted and analyzed by Langmuir and Freundlich isotherm models respectively. It can be seen from Figure 5 that the equilibrium adsorption capacity q_e of rGH increases continuously with the increase of Cr (VI) equilibrium concentration Ce, and gradually tends to saturate. This is because the increase of concentration gradient increases the driving force of adsorption, and the increase of Cr (VI) solution concentration can accelerate the diffusion of Cr (VI) in the solution to rGH surface. At the same time, with the increase of solution temperature from 283.15 K to 323.15 K, the maximum adsorption capacity q_m of rGH for Cr (VI) increased from 85.98 mgg^{-1} to 139.66 mgg^{-1}, and the adsorption capacity increased continuously, indicating that the increase in temperature was more favourable to the adsorption reaction.

Table 2. Isotherm Parameters for the Adsorption of Cr(VI) by rGH.

T（K）	**Langmuir**			**Freundlich**		
	q_m	K_L	R^2	K_F	n	R^2
	mg g^{-1}	L mg^{-1}				
283.15	85.98	0.024	0.993	4.31	1.73	0.981
303.15	100.40	0.034	0.996	7.14	1.82	0.984
323.15	139.66	0.044	0.990	9.52	1.91	0.982

In Table 2, the isotherms of Cr (VI) adsorbed by reduced graphene oxide hydrogels calculated by the two models of Langmuir and Freundlich are listed. It can be seen that compared with the Freundlich model, the isotherms obtained from the Langmuir model are ideal for experimental data, and the correlation coefficients (R^2) of fitting curves are all larger than those of Freundlich models. This shows that the adsorption isotherms of rGH on Cr (VI) are in line with the Langmuir model, and the maximum adsorption capacity qm of rGH on Cr (VI) calculated by Langmuir model at 10, 30 and 50 ° C are 85.98, 100.40 and 139.66 mgg^{-1} respectively. Thus, rGH adsorbs Cr(VI) as a single molecular layer with a limited number of adsorption sites on the surface and adsorption occurs on the homogeneous surface without interaction between the adsorbed Cr(VI) and the unsorbed Cr(VI).

Table 3. Thermodynamic Parameters of Cr(VI) Adsorption on rGH.

T	ln*K*°	*ΔG*°	*ΔH*°	*ΔS*°
(K)		(KJmol^{-1})	(KJmol^{-1})	(J$mol^{-1}K^{-1}$)
283.15	0.55	-1.29	19.74	74.18
303.15	1.06	-2.67		
323.15	1.59	-4.27		

Table 3 lists the results of thermodynamic parameters calculated by the formula at three different temperatures. The negative value of standard Gibbs free energy (△G°) indicates that the adsorption of Cr (VI) by rGH is a spontaneous process, and with the increase of solution temperature, the absolute value of △G° increases and the adsorption capacity increases[12], which may be attributed to the increase of pore size and activation energy of adsorbent surface with the increase of temperature, and the decrease of boundary layer thickness around the adsorbent. The mass transfer resistance of the adsorbate is reduced, corresponding to the results of the adsorption isotherm, and the temperature rise is conducive to the adsorption reaction[13].The standard entropy change (△S°) is 74.18 $jmol^{-1}k^{-1}$, reflecting the increased randomness of the solid-liquid interface during the adsorption of Cr(VI) onto the adsorbent indication, and thus the increased chaos of the system. The standard enthalpy change(△H°) is positive, indicating that the adsorption process of rGH on Cr (VI) is an endothermic reaction. It may be due to the high energy required in the adsorption process to break the hydration sheath structure of metal ions in the dispersion system of hydrated oxide. This is consistent with the phenomenon that the adsorption capacity of rGH to Cr (VI) increases with the increase of solution temperature[14].

Solution pH can change the net surface charge of both the adsorbent and the target adsorbate, which is one of the most important factors affecting the adsorption performance of adsorbent. To investigate the effect of solution pH on rGH adsorption performance, Cr (VI) solution with initial concentration of 60mgl^{-1} was used, and the pH value of the solution was adjusted to the range of 1.0-11.0 respectively. After 60 min of adsorption reaction, samples were taken to determine the residual concentration of different Cr (VI) solutions. The resulting experimental data were plotted as a relationship between solution pH and the equilibrium adsorption amount q_e of rGH.

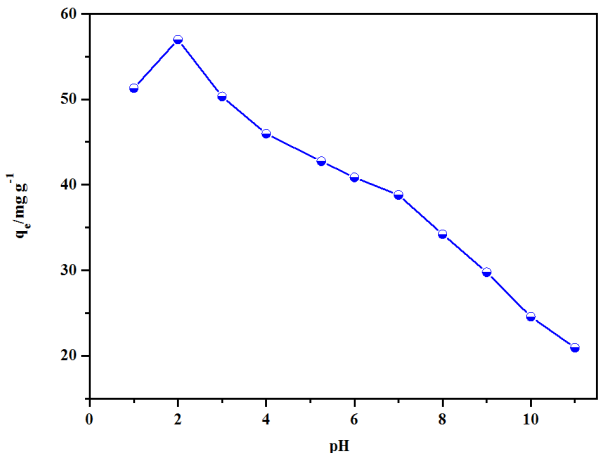

Fig. 6. Effect of removal Cr(VI)on rGH with different initial solution pH.

It can be seen from Fig. 6 that with the increase of pH value, the ability of rGH to adsorb heavy metal ions decreases significantly. In aqueous solution, Cr (VI) mainly exists in five forms: $Cr_2O_7^{2-}$, $HCrO_4^-$, $HCr_2O_7^-$, $CrO_4^{2-}$and H_2CrO_4 .When the pH of the solution is low, the rGH surface is protonated and positively charged. Cr (VI) in the water is quickly removed through

electrostatic attraction to achieve the effect of water purification. When the pH of the solution is > 7.0, the adsorption capacity of rGH decreases significantly, which may be due to the competition between OH^- and CrO_2^{4-}（$Cr_2O_7^{2-}$）on the active sites on the adsorbent surface when the solution pH is under alkaline conditions. At the same time, the rGH surface also has a strong negative charge, resulting in a strong electrostatic repulsion between them. The ability of adsorbed heavy metal ions by reduced graphene oxide hydrogel decreased dramatically.

In addition to various pollutants, there are also a large number of salts in industrial wastewater. Therefore, the ionic strength of solution is also one of the important factors affecting the adsorption performance of adsorbent. The influence of solution ionic strength on the adsorption properties of graphene hydrogels was investigated. The initial concentration was 60 mgL^{-1} Cr (VI) solution and $CaCl_2$ was selected as the representative salt substance. The $CaCl_2$ concentration (i.e. ionic strength) in the solution was 0, 1000, 2000, 5000, 10000, 20000, 30000 and 50000 $mol{\cdot}kg^{-1}$ respectively. The residual concentration of different Cr (VI) solution was determined by taking samples 60 min after the adsorption reaction. The experimental data obtained were plotted as a relationship between $CaCl_2$ concentration in solution and the equilibrium removal rate of graphene hydrogels.

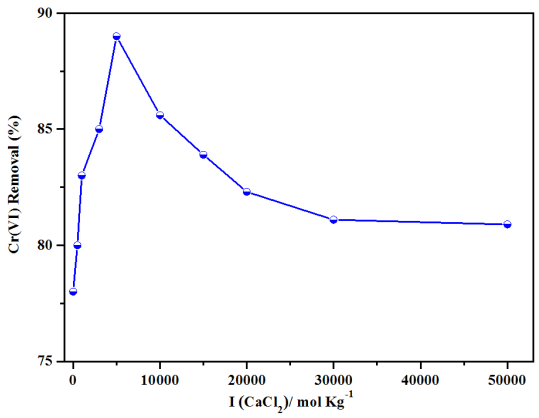

Fig. 7. Effect of removal Cr(VI) on RGH with different initial ionicstrength

It can be seen from Fig.7 that with the increase of $CaCl_2$ concentration in the solution, the adsorption capacity of rGH for Cr (VI) first increases, then decreases, and finally tends to be stable. When the ionic strength of $CaCl_2$ in the solution is lower than 5000 $mol{\cdot}kg^{-1}$, the adsorption capacity of rGH to Cr (VI) increases. This is because $CaCl_2$ in the solution will produce charge shielding effect in the solution, shielding off the electrostatic repulsion between Cr (VI) and rGH surface in the solution and between adsorbed Cr (VI) and non adsorbed Cr (VI), so as to enhance the adsorption between Cr (VI) and rGH surface. When the ionic strength of $CaCl_2$ in the solution is higher than 5000 $mol{\cdot}kg^{-1}$, the adsorption capacity of rGH to Cr (VI) gradually decreases and tends to be stable. This is because too much $CaCl_2$ introduced into the solution will compete with Cr (VI) for the limited active site on the surface of rGH. Due to strong attraction, calcium ions will firmly bind to the surface of rGH to form a tight adsorption layer, and the adsorption site of the original rGH surface for the adsorption of Cr (VI) was occupied by $CaCl_2$, so that the adsorption of Cr (VI) by rGH tended to be flat.

4. Conclusion

The graphene hydrogel rGH prepared by chemical reduction method has unique three-dimensional network structure and pore size distribution. The kinetics and isotherm data can be well described by the pseudo-second-order kinetic model and the Langmuir isotherm, respectively. The adsorption reaction reaches the equilibrium quickly, and the maximum adsorption capacity is 139.66mg.g^{-1}. The thermodynamic parameters indicate that the adsorption is spontaneous and endothermic process. The significant adsorption capacity is mainly attributed to the fact that rGH has nano sheet structure and maintains the surface adsorption characteristics of graphene. Compared with porous and interlayer adsorption materials, rGH avoids the diffusion speed of heavy metal ions in pores and interlayer during the adsorption process, and has the ability of rapid adsorption and enrichment. The π - π action will reduce the competitive adsorption of water and improve the adsorption capacity.

This work is supported by the Key project of National Natural Science Foundation of China-Joint Fund for Regional Innovation and Development [grant number U21A20114] and Hebei Province Natural Science Fund [grant numbers E2020209036].

References

[1] D. Mohan, K.P. Singh., Water Research, 36, 2304 (2002); https://doi.org/10.1016/S0043-1354(01)00447-X

[2] H. Wang, X.Z. Yuan, Y. Wu, X.H. Chen, L.J. Leng, H. Wang, H. Li, G.M Zeng, Chemical Engineering Journal, 262, 597 (2015); https://doi.org/10.1016/j.cej.2014.10.020

[3] Yang Huang, Chaoran Li, and Zhang Lin, ACS Appl. Mater. Interfaces 6, 19766 (2014); https://doi.org/10.1021/am504922v

[4] Hongcai Gao, Yimin Sun, Jiajing Zhou, Rong Xu, and Hongwei Duan, ACS Appl. Mater. Interfaces5, 425 (2013); https://doi.org/10.1021/am302500v

[5] Yang-Xin Yu, ACS Appl. Mater. Interfaces 6, 16267 (2014); https://doi.org/10.1021/am504452a

[6] Marcus A.Worsley, Thang T.Pham, Aiming Yan, Swanee J.Shin, Jonathan R.I.Lee, Michael Bagge-Hansen, William Mickelson, Alex Zettl, Nano 8(10), 11013 (2014); https://doi.org/10.1021/nn505335u

[7] A. Rahim, K. Liaqat, S. Fazil et al., Digest Journal of Nanomaterials and Biostructures16(3), 1147 (2021).

[8] Chen J W, Shi J W, Wang X, et al., Chinese Journal of Catalysis, 34, 621 (2013); https://doi.org/10.1016/S1872-2067(12)60530-0

[9] Y. Li, X. C. Guo, Y. Chen, et al., Digest Journal of Nanomaterials and Biostructures 17(1), 21 (2022).

[10] Huang Z G, Zheng X Y, Lv W, et al., Langmuir, 27(12), 7558 (2011); https://doi.org/10.1021/la200606r

[11] Deng X J, Lü L L, Li H W, et al., Journal of Hazardous Materials, 183, 923 (2010); https://doi.org/10.1016/j.jhazmat.2010.07.117

[12] Y.H. Li, Z. Di, J. Ding, D. Wu, Z. Luan, Y. Zhu, Water Research. 39, 605 (2005); https://doi.org/10.1016/j.watres.2004.11.004

[13] S.H. Asl, M. Ahmadi, M. Ghiasvand, A. Tardast, R. Katal, Journal of Industrial and Engineering Chemistry. 19, 1044 (2013); https://doi.org/10.1016/j.jiec.2012.12.001

[14] V.K. Gupta, D. Pathania, S. Sharma, P. Singh, Journal of Colloid and Interface Science. 401, 125 (2013); https://doi.org/10.1016/j.jcis.2013.03.020